THE ASTROPHYSICAL JOURNAL, 370:237–242, 1991 March 20

DUST AND MOLECULAR PROPERTIES OF THE LOW-OPACITY CLOUD LYNDS 1563

FRANK O. CLARK
Air Force Geophysics Laboratory, GL(AFSC)/OPC, Hanscom AFB, MA 01731-500
R. J. LAUREIJS
Infrared Processing and Analysis Center, California Institute of Technology, MS100-22, Pasadena, CA 91125
AND
LAURI L. WARDELL
Department of Physics, Wellesley College, Wellesley, MA 02181
Received 1990 February 27; accepted 1990 September 4

ABSTRACT

Optical, molecular, and far-infrared data are analyzed for L1563, estimated peak A_b 2.5 mag. The cloud is detected by *IRAS* at 12, 25, 60, and 100 μm, and with CO, ^{13}CO, and H_2CO molecules. A column density comparison yields an estimate of the temperature of the classical dust grains of 15.6 K (± 1 K), while the color temperature derived from the ratio $I(60)/I(100)$ is 26 K. Both dust and color temperatures decrease toward the cloud center. ^{13}CO and H_2CO spectral lines are detected above a threshold in $I(100)$. $I(12)$ and $I(25)$ increase with $I(100)$ only in the outer regions of the cloud. The ratio of $^{13}CO/^{12}CO$ integrated intensity rises toward the cloud center by 10.

Subject headings: interstellar: grains — interstellar: molecules — nebulae: individual (Lynds1563)

1. INTRODUCTION

The regions of optical obscuration, L1562 and L1563, form an elongated cloud located at high Galactic latitude ($l = 187°$, $b = -16°$). Both regions are listed by Lynds (1962) as opacity class 5 objects. In an infrared-selected sample of high-latitude clouds that are well isolated from their surroundings, L1563, concentrated on here, is one of the lowest opacity objects for which a variety of molecular spectral lines could be detected.

In the present paper we investigate the relationships between molecular spectral lines and infrared emission. The cloud L1563 can be classified as intermediate between diffuse and dark clouds, sometimes referred to as translucent clouds. As a result of the extensive diffuse envelope around L1563, processes that otherwise occur in a transition region of limited spatial extent in dense clouds can now be examined with sufficient resolution.

The cloud has been studied using published data on field stars, *IRAS* HCON3 sky flux images, $J = 1$–0 emission lines of CO (^{12}CO) and ^{13}CO, and $1_{1,0}$–$1_{1,1}$ absorption lines of H_2CO. *IRAS* and CO data were obtained for the entire complex, L1562/L1563. L1562 was not observed with H_2CO. A detailed analysis concentrates on the more regular southern half of the complex, L1563.

2. OBSERVATIONS

2.1. *IRAS*

The *IRAS* HCON3 sky flux images (*IRAS Explanatory Supplement* 1985) were reduced using techniques described elsewhere (Zhang et al. 1988). These images are shown in Figure 1. For analysis, the 12, 25, and 60 μm images were smoothed to the nominal 6′ resolution of the 100 μm images.

2.2. *Gornergrat*

Emission lines of ^{12}CO and ^{13}CO were obtained during observing runs in 1987 June and 1988 July with the University of Cologne[1] 3 m telescope using a single-channel Cassegrain cooled Shottky barrier mixer (Winnewisser et al. 1986). The half-power beamwidth was 4′ on the 3 mm $J = 1 \rightarrow 0$ spectral line of CO. An AOS spectrometer was used with a frequency resolution of 66 KHz. Pointing was accomplished by observing the planets Jupiter and Venus. The system temperature was about 450 K. The intensity calibration was automatically obtained with hot and cold vane loads. This calibration was checked by frequent comparison with the emission from Orion (OMC-1) and the L1563 source center. The 1987 data were taken with full beam 4′ spacing; the 1988 data were oversampled with 2′ half-beam spacing in accordance with *IRAS* sky flux data. All data were taken in such a way that no regridding was required. The Gornergrat CO images were smoothed to 6′, the nominal spatial resolution of the 100 μm *IRAS* sky flux images. The beam efficiency was 0.65.

2.3. *NRAO*

The 6 cm ($1_{1,0} \rightarrow 1_{1,1}$) spectral line of formaldehyde was observed in 1989 August on the NRAO[2] 140 foot (43 m) antenna using a dual-channel prime-focus HEMT receiver with nominal system temperatures of 28 and 30 K, and an autocorrelation spectrometer with velocity resolution of 0.15 km s^{-1}. Pointing was accomplished by observing strong continuum sources throughout the run. Calibration was done with a noise tube. These data were oversampled to the same 2′ grid as the *IRAS* and CO data, one-third of the nominal 6′ beam size. The spectral line was detected over most of L1563. A beam efficiency of 0.6 was used.

[1] The KOSMA 3 m radiotelescope at Gornergrat-Süd observatory is operated by the University of Cologne and supported by the Deutsche Forschungsgemeinschaft (DFG) through grant SFB-301, as well as by special funding from the Land NRW. The observatory is administered by the Hochalpine Forschungstationen, Jungfraujoch und Gornergrat, Bern.

[2] The National Radio Astronomy Observatory is operated by Associated Universities for Research in Astronomy, Inc., under contract with the National Science Foundation.

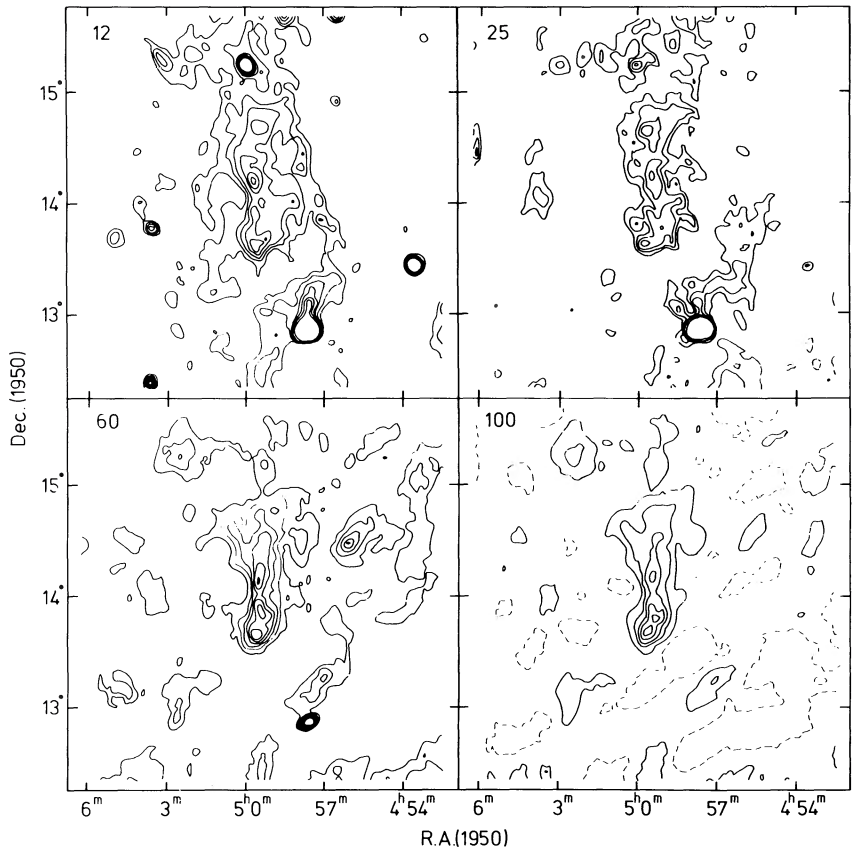

FIG. 1.—*IRAS* 12, 25, 60, and 100 μm sky flux map from HCON3. Contours (in MJy sr^{-1}) are respectively from 0.15 in steps of 0.15; from 0.2 in steps of 0.2; from −0.25 in steps of 0.5; and from −2.5 in steps of 2.5. L1562 is at R.A. = 4^{h}59^m, decl. = 14°12′; L1563 at R.A. = 4^{h}59^m.3, decl. = 13°48′; and HD 31764 at R.A. = 4^{h}56^m.1, decl. = 14°28′.

3. DISTANCE TO THE CLOUD

The distance to the cloud was estimated by surveying the literature for all photometric and spectroscopic data on stars within 3° of the cloud. This produced nine stars with spectroscopic distances. These stars are shown in Table 1, and their extinction, A_V, is displayed as a function of distance in Figure 2. The uncertainty associated with spectroscopic parallax is of order 20%. There is an appreciable increase in field extinction between the stars at 83 and 177 pc, suggesting the presence of an extinction cloud in this interval.

The star HD 31764, a B7 V visual binary star (m = 6 mag), shows associated extended 60 μm emission (Fig. 1). The infrared emission indicates the presence of dust in the immediate vicinity of the star. Given the spectral class and luminosity of HD 31764, the radius at which local heating from the star falls to that of the interstellar radiation field is 7′ (Mathis, Mezger, & Panagia 1983). The estimated size is in agreement with the observed size of the region. A CO emission line of 1.4 K was detected at this position at 8.1 km s^{-1} LSR, the same velocity as the cloud. On the basis of the presence of localized 60 μm emission consistent with expected heating from this star, and on the identical CO line velocities, we conclude that HD 31764 is in actual proximity to the cloud, and the stellar distance

TABLE 1

NEARBY STARS WITH SPECTROSCOPIC DISTANCES

HD	$m(v)$	Spectral Type	A_V (mag)	R (pc)
31966.....	6.6	G5 V	−0.12	22
32850.....	7.7	K0 V	−0.03	24
33276.....	4.9	F2 IV	−0.19	35
32347.....	9.0	G8 V	−0.03	52
32549.....	4.7	B9 (A0p)	−0.03	83
31764.....	6.1	B7 V	0.51	177
31373.....	5.7	B8 III	0.34	210
286295.....	10.1	A5 V	0.37	368

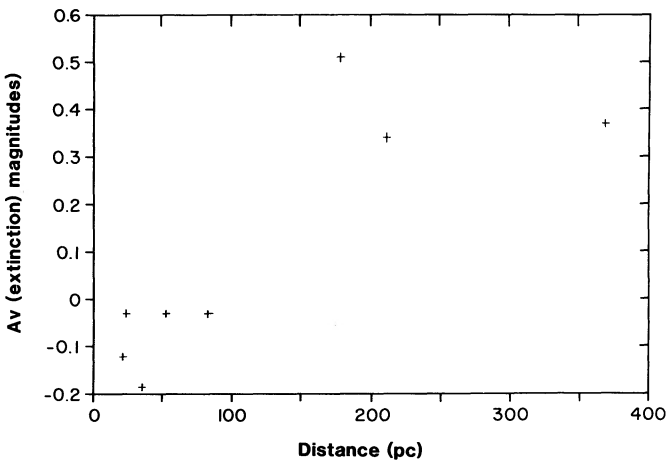

FIG. 2.—Extinction (A_V) (mag) of stars within 3° of L1562 and L1563, vs. distance (pc) calculated from spectroscopic parallax.

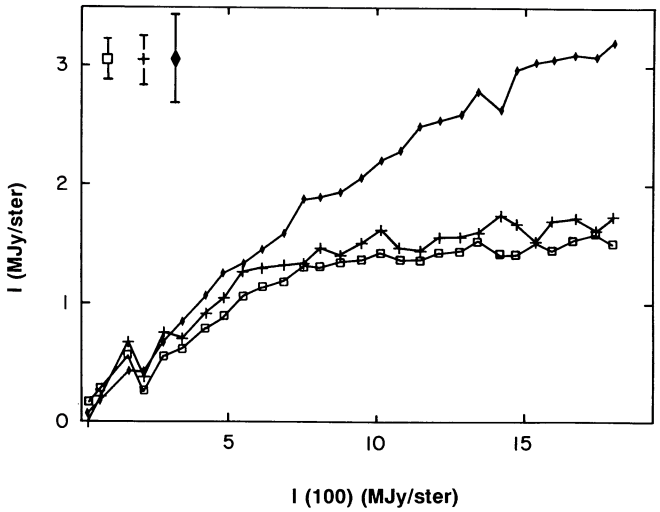

FIG. 3.—$I(12)$ times 2.5, $I(25)$ times 2, and $I(60)$ vs. $I(100)$, all in MJy sr^{-1}. $I(12)$, $I(25)$, and $I(60)$ have been smoothed to the resolution of $I(100)$.

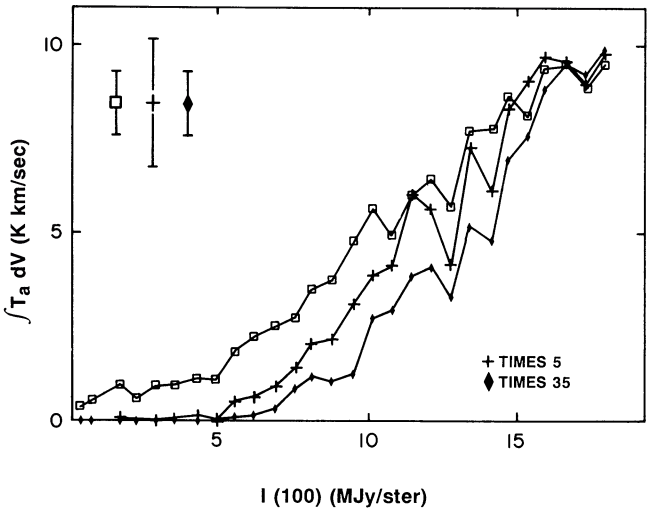

FIG. 4.—$\int T_a dV$ (K km s^{-1}) of ^{12}CO (*squares*), ^{13}CO times 5 (*plus signs*), and $-H_2CO$ times 35 (*diamonds*), vs. $I(100)$ (MJy sr^{-1}) on a pixel-to-pixel basis. All molecular data have been oversampled to 2′ pixels like the *IRAS* sky flux images, and the CO data smoothed to the resolution of the *IRAS* data. The bar shows a formal statistical 1 σ error.

should be the cloud distance. The stellar distance of 180 pc is adopted for the cloud. This cloud is therefore a part of the Gould Belt/Taurus dark cloud complex.

4. OBSERVATIONAL CHARACTERISTICS OF THE CLOUD

4.1. *Infrared Data*

Figure 1 reveals the detection of the cloud at all four *IRAS* bands. The morphology of the cloud is that of a double-peaked source, with the northern component (L1562) more diffuse than the southern (L1563).

Figure 3 shows $I(12)$, $I(25)$, and $I(60)$ versus $I(100)$. Both $I(12)$ and $I(25)$ exhibit a rise up to a level of approximately 8 MJy sr^{-1} and are flat thereafter. $I(60)$ exhibits a steadily decreasing slope with respect to $I(100)$, indicating a declining 60/100 μm ratio with increasing $I(100)$.

4.2. *Molecular Data*

CO and ^{13}CO molecular lines are weaker in the northern half of the cloud, L1562. In the southern portion (L1563) formaldehyde was detected in absorption against the 3 K background radiation. L1562 was not observed with formaldehyde, because of the weaker CO lines there. The remainder of the analysis will focus on L1563, where these data may be intercompared.

A set of pixel-to-pixel correlation diagrams of CO, ^{13}CO, and H_2CO versus $I(100)$ is shown in the three curves in Figure 4. The data have been binned at regular intervals in $I(100)$ for clarity. The correlation diagrams display similar trends: the molecular lines are detected after a threshold at $I(100)$, and $\int T_a dV$ increases with increasing $I(100)$. $I(100)$ is taken as a tracer of column density of the cloud. A similar relationship but with a threshold of 6 MJy sr^{-1} is observed between ^{13}CO and $I(100)$ (Fig. 4, *plus signs*). A threshold of 8 MJy sr^{-1} is apparent between H_2CO and $I(100)$ (Fig. 4, *diamonds*).

Figure 5 shows the ratio of $\int T_a dV$ of ^{13}CO/^{12}CO, which rises toward the cloud center.

5. DISCUSSION OF PHYSICAL CHARACTERISTICS OF LYNDS 1563

The radial velocity of HD 31764 was measured by Evans (1979) as -6.7 km s^{-1} LSR, indicating an appreciable difference between the stellar photospheric (-7 km s^{-1}) and gas velocities ($+8$ km s^{-1}). The difference suggests that the star formed elsewhere and drifted into the cloud complex. The proper motion of the star taken from the SAO catalog (1971) yields a transverse velocity of 5 km s^{-1} east and 14 km s^{-1} south at a distance of 180 pc. Thus the space motion of the star is toward the Sun and toward an approximately grazing approach to the southernmost extremity of L1563. These results support the general conclusion previously reached by Ambarzumian & Gordeladse (1937), that the proximity of the majority of stars near clouds is fortuitous, reached from statistical arguments.

The 12 and 25 μm morphologies are offset from those at 60 and 100 μm, in the direction of the Galactic plane to the east (Fig. 1). This suggests that the 12 and 25 μm carriers respond to the direction of the heating from the local interstellar radiation field. HD 31764, which is associated with the periphery of L1562, exhibits associated $I(60)$ and $I(100)$ in its immediate vicinity, but not $I(12)$ or $I(25)$. The star is presumably lying in the very outermost envelope of the cloud where the volume

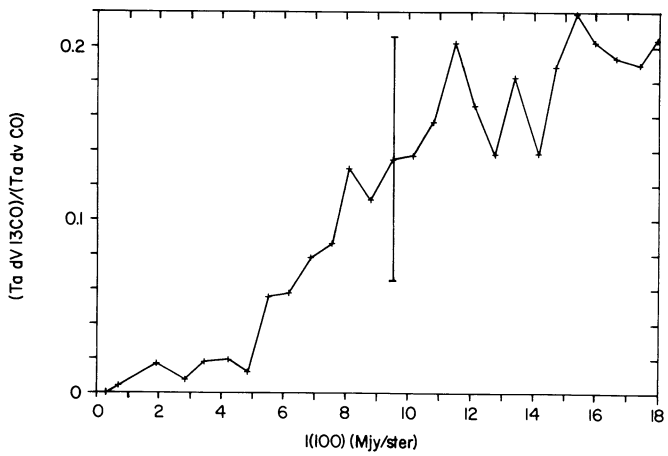

FIG. 5.—$\int T_a dV$ of ^{13}CO divided by the $\int T_a dV$ of CO in K km s^{-1}, vs. $I(100)$ (MJy sr^{-1}) on a pixel-to-pixel basis.

density is low, estimated as a few tens of cm^{-3}. The $I(60)$ and $I(100)$ emission suggests local stellar heating of the larger grains out to a distance from the star of several arcminutes. Perhaps a B7 V star, effective temperature 13,500 K, which by the Wien displacement law would peak near 0.2 μm wavelength, has insufficient ultraviolet to excite the carriers of the 12 and 25 μm emission.

The CO data may be used to estimate the column density of the cloud. A large velocity gradient (LVG) code was initially used to analyze the cloud emission, but the results for L1563 were identical to the relation suggested by Liszt (1982). The agreement confirms that the CO emission lines are optically thin throughout the cloud, consistent with the close correlation between the three species. The mass of L1563 is found to be 140 $M_\odot$ ($\pm$20 $M_\odot$), with an implied average volume density of $n_{H_2} = 5\ (1\text{–}6) \times 10^3\ cm^{-3}$. The estimate of the volume density promoted a successful search for the 6 cm formaldehyde absorption line.

5.1. *Temperature of Large Dust Grains*

The CO column density may be combined with $I(100)$ to estimate the temperature of the classical component of the dust. This technique has previously been applied by Terebey & Fich (1986) using H I column densities, and by Weikard & Duvert (1988), who used ^{13}CO column densities. The relationships and parameters suggested by Hildebrand (1983) were applied to obtain a cloud dust temperature of 15.5 K (13–16) averaged over the area of L1563, where the range of uncertainty includes the allowable range in distance, dust emissivity, background in the $I(100)$ maps, CO/H_2, and range of dust parameters listed by Hildebrand.

Figure 6 shows the dust temperature obtained as a function of $I(100)$, where the latter can be regarded as an equivalent to cloud radius. T_d declines from 15 K at the cloud edge to 14 K near the cloud center. These values would be approximately 1 K smaller if an emissivity proportional to λ^{-2} had been assumed for the dust, but the trend would be unchanged. Also shown is the color temperature, T_c, derived from $I(60)/I(100)$, which exhibits a decline from 28 to 25 K. The 60 μm/100 μm color temperature is some 10 K larger than the actual temperature of the large dust grains.

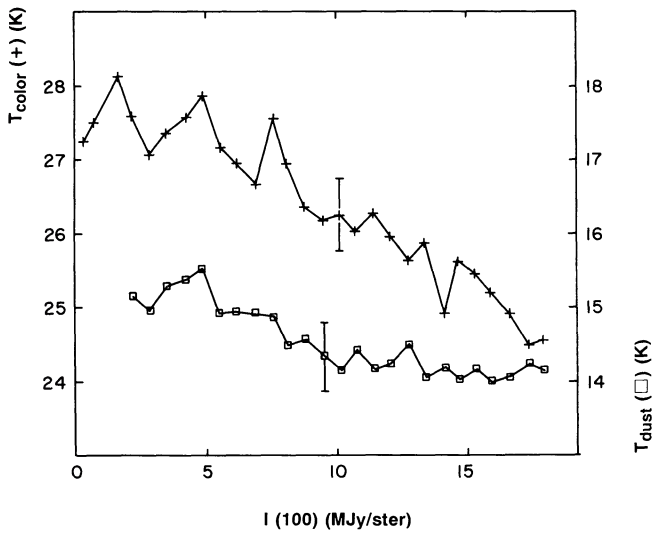

FIG. 6.—*Upper curve* (*plus signs*): T_c (K) [from $I(60)/I(100)$: emissivity varying with λ^{-1} was assumed] vs. $I(100)$ (MJy sr^{-1}). *Lower curve* (*squares*): T_d (K) (calculated temperature of large grains [from CO]) vs. $I(100)$. All data have been smoothed to the spatial resolution of $I(100)$.

Despite the similar trends, the two determinations show a significant discrepancy in temperature of about 10 K. The values of T_c and T_d can only be matched either by changing the gas-to-dust ratio by a factor of 90, or alternatively, by changing the dust emissivity at 100 μm by a factor 1/90. Although the uncertainties in the canonical values of both the gas-to-gas ratio and the 100 μm emissivity are large (Hildebrand 1983; Draine 1990), our derived factors are too substantial to account for a general explanation of the temperature discrepancy. The most likely interpretation is that a significant part of the 60 μm emission is due to a population of grains which has properties different from those of the grains emitting at 100 μm. This implies that T_c as derived from the ratio $I(60)/I(100)$ cannot be considered as a physically meaningful measure of the temperature of the grains emitting at 60 or 100 μm. In addition, Figure 3 illustrates that both $I(12)$ and $I(25)$ exhibit a markedly different behavior compared with that of $I(60)$, evidence that the grains emitting at 60 μm are not to be identified with the grains emitting at 12 or 25 μm either.

There are other indications in the literature that the 60 μm emission detected by *IRAS* is not due to the same grain component as that producing the 100 μm emission:

1. Although a typical diffuse $I(60)/I(100)$ T_c in the solar vicinity is of order 26 K, dust models are unable to produce grain temperatures this high (Cox, Krugel, & Mezger 1986).
2. By comparing H I and $I(100)$ column intensities, Terebey & Fich (1986) conclude that T_d in the diffuse interstellar medium is 18 K, while the color temperature is of order 26 K.
3. Laureijs, Chlewicki, & Clark (1988) find that $I(60)/I(100)$ *rises* before it fails as the cloud center is approached.

It is also clear that, whatever the nature of these unknown 60 μm emitters, they track the $I(100)$ far-infrared emission better than either $I(12)$, $I(25)$, or molecular lines. Therefore, $I(60)$ behaves as if it were thermal emission from an independent grain component that absorbs roughly in the same wavelength range as the 100 μm emitters. This is consistent with a population of smaller grains at a higher constant temperature. The decline in T_c in Figure 6 is greater that of T_d (Fig. 6), although changes in CO abundance could affect the slope in T_d. Possible interpretations are that the 60 μm emitters are somewhat more strongly affected by the cloud opacity than the large dust grains responsible for the $I(100)$ emission, or that the 60 μm emitters are being depleted. The former interpretation implies that the 60 μm emitters may be heated by slightly bluer radiation than the large dust grains.

5.2. *Inferred Fractional Abundances*

The column density in the outer environs of L1563 was estimated with $I(100)$, since the higher signal-to-noise and good sampling are superior to those afforded by molecular data. $I(100)$ was converted to column density using the temperature distribution obtained from the comparison between $I(100)$ and CO, supplemented in the outer edge of the cloud by imposing the dust temperature at zero extinction derived by Terebey & Fich (1986) for the diffuse interstellar medium (18 K). The result is shown in Figure 7, as ^{12}CO/column, ^{13}CO/column, and H_2CO/column versus normalized column density. ^{12}CO is flat over the inner portion of the cloud, consistent with the computational method, rising precipitously in the outermost points. The signal-to-noise ratio in the molecular

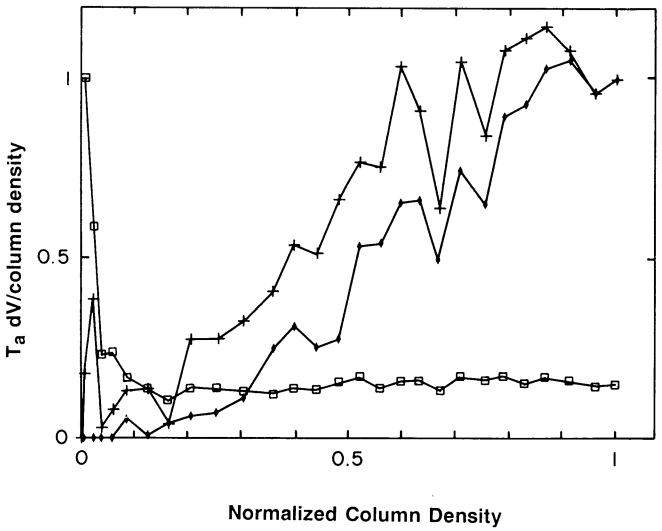

FIG. 7.—$\int T_a dV$ (arbitrary units), of ^{12}CO (*squares*), ^{13}CO times 5 (*plus signs*), and $-H_2CO$ times 35 (*diamonds*), all divided by column density, vs. normalized column density.

data is sufficient to lend credence to the reality of this effect. If real, then this rise most probably represents the increase in gas kinetic temperature predicted to occur at the cloud edge in models. Clavel, Viala, & Bel (1978) predict a rise to 15–25 K, while Falgarone & Puget (1985) predict values as high as 50–100 K at the edge of clouds. The ^{13}CO data also hint at a rise, but the trend is of less significance, since the detections are at the 2 σ level. H_2CO was undetectable in this region. If it is assumed that $\int T_a dV$ is linearly proportional to molecular column density over the regime sampled, then ^{13}CO exhibits an inferred 10 times increase in fractional abundance, while H_2CO exhibits a 40 times increase in fractional abundance.

5.3. *Ratio of* ^{13}CO to CO

The linearity between CO and both ^{13}CO and H_2CO, and the agreement in column density estimates, indicate that CO is effectively optically thin over the range of observation. Therefore, the ratio of integrated intensities of $^{13}CO/CO$ shown in Figure 5 may be taken to represent an increase in abundance ratio of these isotropic species of a factor greater than 10. This result is in agreement with the predictions of Langer (1985), and involves both isotropic fractionation and self-shielding effects. The H_2CO data show a corresponding increase in the ratio of line strength to hydrogen density, implied to represent an increase in fractional abundance of a factor of 40 from the edge to the center.

5.4. 12 *and* 25 μm *Emission*

The dust temperature map calculated above may be used to estimate cloud properties related to shorter wavelength emission. For a cloud heated by an external radiation field, I_0, the energy absorbed will be equal to that emitted:

$$\int \sigma Q_{\rm abs} I_0 e^{-\tau} d\Omega = \int \sigma Q_{\rm em} B(\lambda, T_d) d\Omega \ , \qquad (1)$$

where σ represents the geometrical cross section of the grains, $Q_{\rm abs}$ and $Q_{\rm em}$ represent the "efficiency" of the grains at the absorbing wavelength and emitting wavelength, respectively, τ is opacity at the effective heating wavelength, B is the Planck function, λ is wavelength, T_d is dust temperature, and Ω is solid angle. The opacity, τ, includes the effects of absorption, scattering, and reradiation. If the assumption is made that σ is the same for absorption and emission, that both Q's may be represented by average quantities that do not change within the cloud, and that I_0 is a constant, then determination of an integrated T_d (above) is equivalent to an estimate of τ.

In Figure 8 is shown $I(12)$ and the above-derived opacity, scaled to match the peak $I(12)$. One interpretation of the agreement between the two is that $I(12)$ is more sensitive to the source of heating radiation than to the total column density of the cloud. In other words, the 12 and 25 μm emission is consistent with a uniform-density shell of emitters around the cloud. This interpretation suggests that the abundance of the 12 and 25 μm emitters declines as density increases in the cloud.

6. CONCLUSIONS

Apparently, L1563 has had no star formation in the past and has no *IRAS* point sources in it at the present time. The star HD 31567 is expected to have minimal effect on the cloud at its projected distance, aside from slight local heating, which is confirmed by the *IRAS* data. The correspondence between molecular probes and dust emission in this low-opacity cloud is in good agreement with model expectations.

The calculated temperature of the large dust grains is lower than the apparent color temperature, providing evidence that a large fraction of the 60 μm emission is not due to these grains. $I(60)$ most closely correlates with $I(100)$ and not with $I(12)$ and $I(25)$, suggesting a second thermal component of dust emission. Both the temperature of the dust grains and the color temperature derived from $I(60)/I(100)$ decline from the edge to the center of the cloud.

There is a clear depiction in the data of the threshold of detection in the $1_{1,0}$–$1_{1,1}$ 6 cm spectral line of formaldehyde, beyond which the line is undetectable. This spectral line requires a minimum volume density of colliding particles to excite it into absorption against the 3 K background. It may be concluded that L1563 is a centrally condensed cloud, and the threshold of detection delineates the minimum volume required to refrigerate this spectral line below 3 K. For a non-

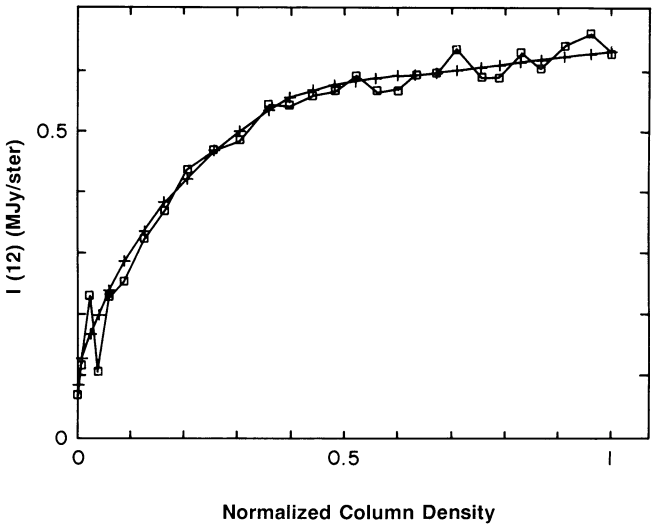

FIG. 8.—$I(12)$ (MJy sr^{-1}) (*squares*; MJy sr^{-1}) and derived large grain heating opacity [*plus signs*; arbitrary units, scaled to $I(12)$; see text] vs. normalized column density.

centrally condensed object, this spectral line may not be detectable for a far-infrared surface brightness of 8 MJy sr^{-1}.

We note in passing that the data are consistent with the 12 and 25 μm carriers, exhibiting a decline in abundance at approximately the same region in the cloud where the molecules begin to exhibit an increase in abundance, approximately $I(100) = 6$ MJy sr^{-1}.

The integrated line profile of $^{13}CO/^{12}CO$ increases by 10 from the edge to the center of the cloud, consistent with abundance predictions of these species.

Both 12 and 25 μm radiation appear to reflect the decline in external heating radiation as it penetrates the cloud, but are less responsive to cloud column density.

This centrally condensed, regular-geometry object should be an excellent cloud for future modeling and for future higher spatial resolution observations, since it has at least one moderately dense core.

We stress the importance of a high surface accuracy, small-aperture telescope with state-of-the-art receivers and spectrometers for study of clouds of large angular size. The required observational data would have required heroic amounts of time on a large telescope with a small beam size.

This research was partially supported by NATO grant 0093/88 and by NASA grant 055-89 to F. O. C. at the University of Kentucky. F. O. C. especially acknowledges Professor Dr. Winnewisser for generously granting observing time on the very fine University of Cologne telescope on the Gornergrat, for very able assistance from many staff and students at the University of Cologne during and after the observations, and for summer support during a stay at the University of Cologne during the summer of 1988. R. J. L. acknowledges an NRC Postdoctoral Research appointment. Radial velocity measurements of HD 31764 were obtained from the SIMBAD data retrieval system, data base of the Strasbourg, France, Astronomical Data Center.

REFERENCES

Ambarzumian, V., & Gordeladse. 1937, Bull. Abastumani Obs., 2, 37
Clavel, J., Viala, Y. P., & Bel, N. 1978, A&A, 65, 433
Cox, P., Krugel, E., & Mezger, P. G. 1986, A&A, 155, 380
Draine, B. T. 1990, in The Interstellar Medium in Galaxies, ed. H. A. Thronson & J. M. Schull (Dordrecht: Kluwer), in press
Evans, D. S. 1979, in IAU Symposium 30, Determination of Radial Velocities and Their Applications, ed. A. H. Batten & J. F. Heard (New York: Academic), 57
Falgarone, E., & Puget, J. L. 1985, A&A, 142, 157
Hildebrand, R. H. 1983, QJRAS, 24, 267
IRAS Catalogs and Atlases: Explanatory Supplement. 1985, ed. C. A. Beichman, G. Neugebauer, H. J. Habing, P. E. Clegg, and T. J. Chester (NASA RP-1190; Washington DC: GPO)
Langer, W. D. 1985, in Les Houches Session XLI, Birth and Infancy of Stars, ed. R. A. Lucas, A. Omont, & R. Stora (Amsterdam: North-Holland), 279
Laureijs, R. J., Chlewicki, G., & Clark, F. O. 1988, A&A, 192, L1
Liszt, H. S. 1982, ApJ, 262, 198
Lynds, B. T. 1962, ApJS, 7, 1
Mathis, J. S., Mezger, P. G., & Panagia, N. 1983, A&A, 128, 212
Matsakis, D. N. 1979, ApJ, 234, 861
Smithsonian Institution. 1971, Smithsonian Astrophysical Observatory Star Catalog (Smithsonian Inst. Pub. 4652)
Terebey, S., & Fich, M. 1986, ApJ, 309, L73
Weikard, H., & Duvert, G. 1988, in The Physics and Chemistry of Interstellar Molecular Clouds, ed. G. Winnewisser & J. T. Armstrong (Lecture Notes in Physics, Vol. 331; Berlin: Springer-Verlag), 130
Winnewisser, G., et al. 1986, A&A, 167, 207
Zhang, C. Y., Laureijs, R. J., Clark, F. O., & Wesselius, P. R. 1988, A&A, 199, 170